

Structural Characterization of Native and Modified Encapsulins as Nanoplatfoms for *In Vitro* Catalysis and Cellular Uptake

Rindia M. Putri,[†] Carolina Allende-Ballesteros,[‡] Daniel Luque,^{‡,§} Robin Klem,[†] Katerina-Asteria Rousou,[†] Aijie Liu,[†] Christoph H.-H. Traulsen,[†] W. Frederik Rurup,[†] Melissa S.T. Koay,[†] José R. Castón,^{‡*} Jeroen J.L.M. Cornelissen^{†*}

[†]Department of Biomolecular Nanotechnology, MESA+ Institute for Nanotechnology, University of Twente, 7500 AE Enschede, The Netherlands

[‡]Department of Structure of Macromolecules, Centro Nacional de Biotecnología/CSIC, Cantoblanco, 28049 Madrid, Spain

[§]Centro Nacional de Microbiología/Instituto de Salud Carlos III, 28220 Majadahonda, Madrid, Spain

*Correspondence to: j.j.l.m.cornelissen@utwente.nl; jrcaston@cnb.csic.es

S1. Native encapsulin (DyP-E) response to variation of ionic strength

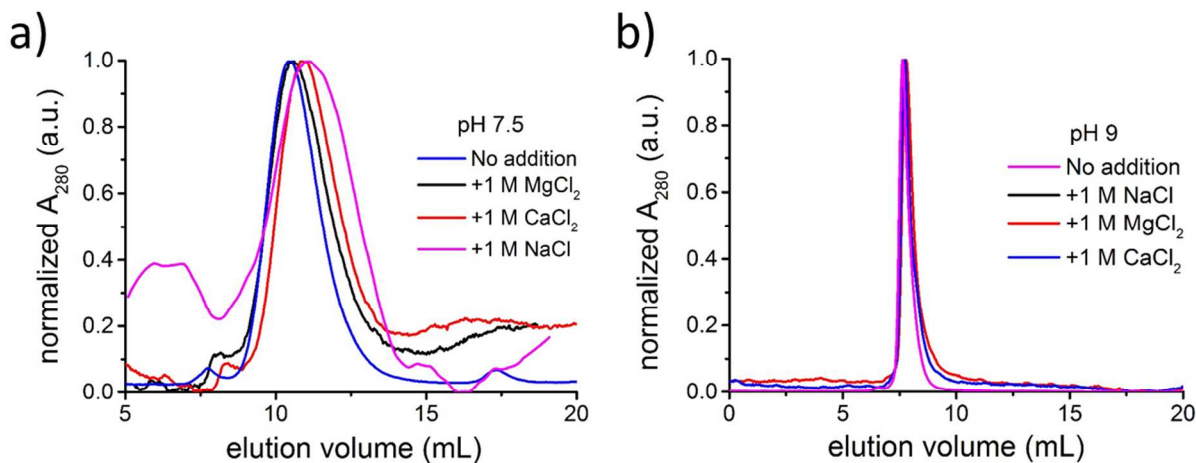


Figure S1. Characterization of encapsulin at different ionic strength. (a) Size-exclusion profiles of native encapsulin at native pH (pH 7.5) in the presence of different salts monitored at $\lambda = 280$ nm, revealing a single peak of encapsulin ($V = 10 - 12$ mL) for each profile. (b) Size-exclusion profiles of native encapsulin at elevated pH (pH 9) in the presence of different salts monitored at $\lambda = 280$ nm, revealing a single peak of encapsulin ($V = 9$ mL) for each profile.

S2. Native encapsulin (DyP-E) response to addition of organic solvents

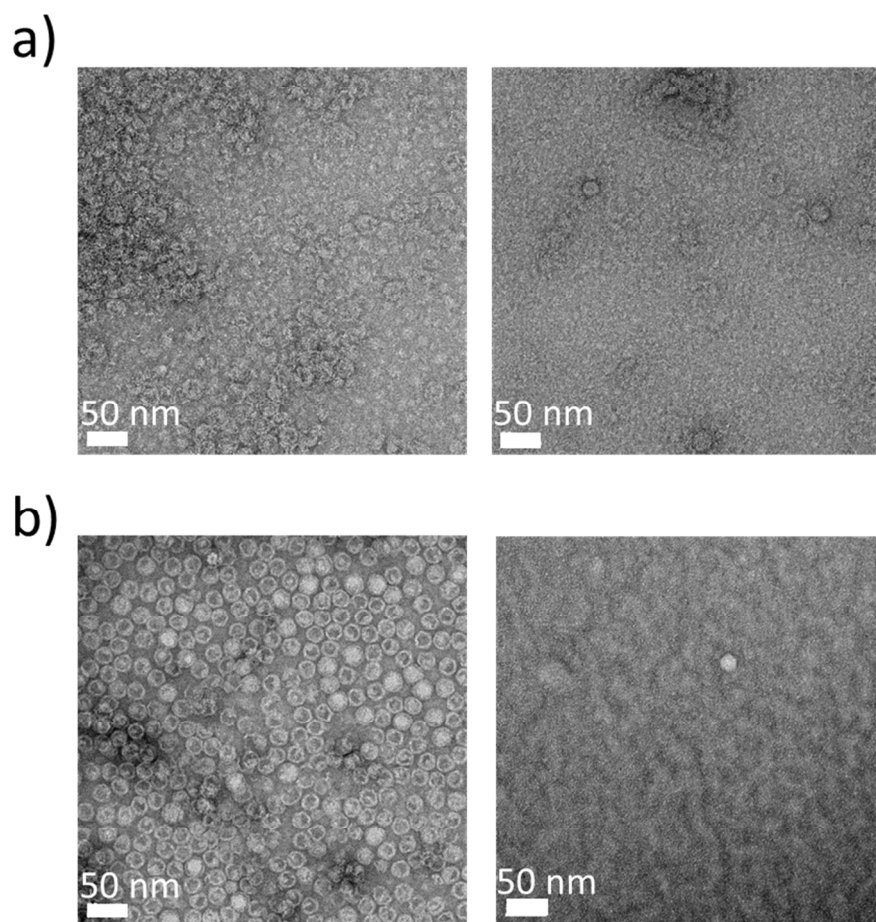


Figure S2. Characterization of encapsulin in the presence of organic solvent. TEM images of native encapsulin (size around 20 nm) in the presence of (a) DMSO (left: 20% right: 40%) and (b) ethanol (left: 20% right: 40%). All samples were in Tris-HCl buffer pH 7.5.

S3. Analyses of empty encapsulin (nl-E)

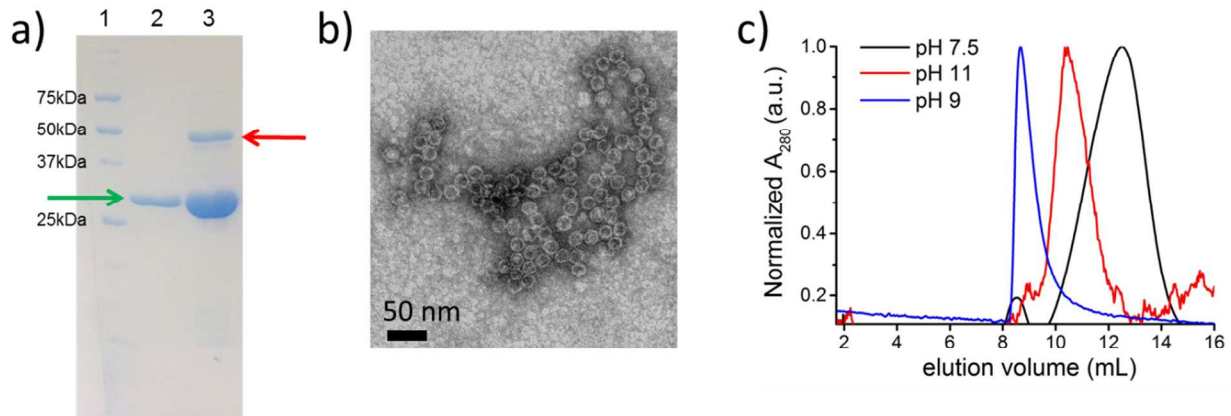


Figure S3. Characterization of empty encapsulin. (a) Denaturing gel electrophoresis revealing the encapsulin band (~28 kDa, green arrow) and the cargo DyP band (~50 kDa, red arrow). Lane 1 corresponds to protein marker and lane 2 and 3 correspond to empty (nl-E) and native (DyP) particles, respectively. (b) TEM image of nl-E at pH 7.5. (c) Size-exclusion profiles of nl-E at pH 7.5 (black line), pH 9 (blue line) and pH 11 (red line).

S4. Cascade catalysis of GOx and surface-immobilized DyP-E

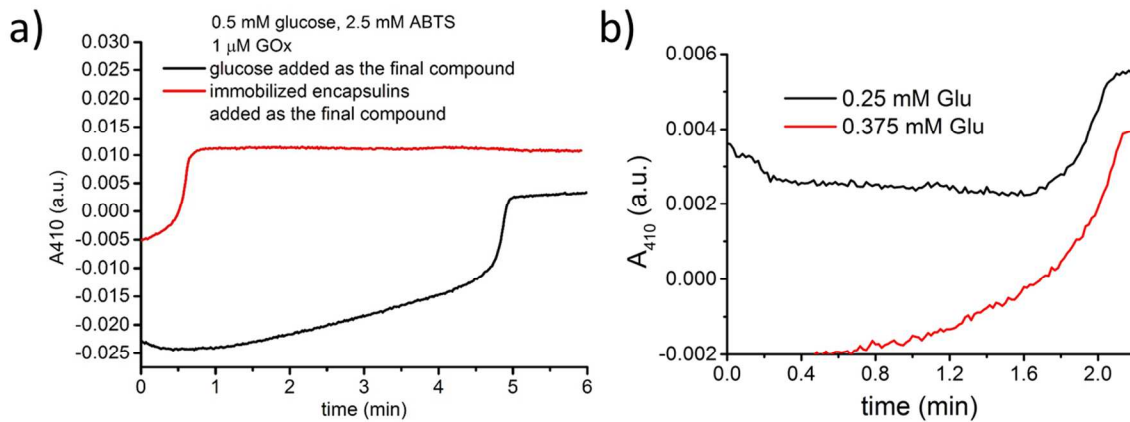


Figure S4. Different order of addition resulting in different “lag” phase. (a) At a fixed concentration of all substrates and enzymes, the “lag” phase is longer if the substrate glucose is as the final component to the system (black line, reaction starts at $t = 5$ min). On the contrary, if the surface-immobilized encapsulin is added to the mixture of GOx-glucose, the “lag” phase is significantly shortened (red line). Two different experiments (red and black lines) result in the same value of slope dA/dt (i.e., 0.096), indicating the reproducibility of the assay. (b) Catalytic assay at lower concentration of substrate glucose, i.e., using 0.25 mM (black line) and 0.375 mM (red line) glucose.

Table S1. Reaction rates derived from dA_{410}/dt at different substrate concentrations

[Glu] (mM)	dA_{410}/dt	v ($\mu\text{M}/\text{min}$)
0.25	0.016	0.45
0.38	0.017	0.46
0.5	0.096	2.67
2.5	0.041	1.14
3.2	0.056	1.57
5.0	0.066	1.83

S5. Stability of modified encapsulin (TFP-E) over time

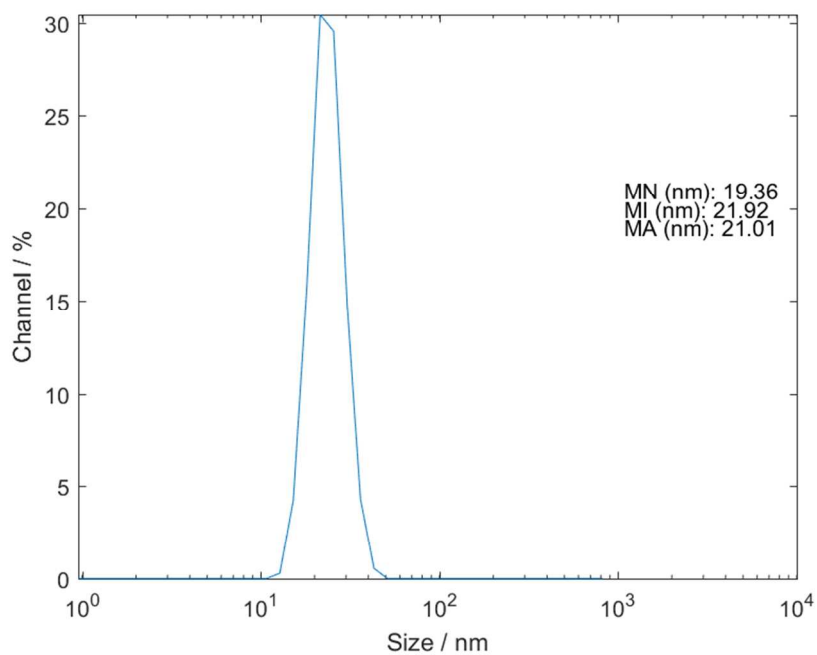


Figure S5. Characterization of modified encapsulin with a fluorescent protein TFP cargo (TFP-E). Size distribution of TFP-E particles over five years of storage at 4°C , revealing the presence of intact particles with the expected size of around 20 nm.